Cooperative Control for Moving-Target Circular Formation of Nonholonomic Vehicles

Xiao Yu, *Student Member, IEEE*, and Lu Liu, *Senior Member, IEEE*

***Abstract*—This note investigates the problem of moving-target circular formation of nonholonomic vehicles, such that the controlled vehicles orbit around a target moving with a time-varying velocity and maintain even spacing along the common circle. A cooperative controller is developed for each vehicle via local measurements only. The topology of the sensor graph may dynamically switch based on the relative positions between vehicles and the target. Moreover, measurements in the local Frenet-Serret frame of each vehicle rather than in a global coordinate frame are used. Finally, the effectiveness of the proposed controller is verified by the simulation results of an example.**

***Index Terms*—Cooperative control, moving-target circular formation, nonholonomic vehicles.**

I. Introduction

Over the last decade, tremendous research effort has been devoted to formation control of multi-agent systems [1]. In particular, circular formation where multiple nonholonomic vehicles orbit around a target along a common circle, has attracted much attention recently due to its wide applications [2]. For example, formations of multi-vehicle systems under cyclic pursuit were studied in [3, 4]. In [5, 6], the authors provided comprehensive investigations on circular formation of vehicles under all-to-all and limited communication. In [7], limited visibility of onboard sensors for vehicles was taken into account. In [8], a hybrid control law via local measurements was developed. In [9, 10], collective circular motion was addressed with a jointly connected graph condition. In [11], a hierarchical design approach was proposed for multiple dynamic unicycles. In [12], control schemes using only local bearing measurements were developed.

However, in aforementioned works, the center of circular formation is assumed to be *stationary* no matter it is a priori given or dependent on initial positions of the vehicles. These control approaches cannot be directly extended to the case where the center is moving.

Moving-target circular formation of vehicles modeled by single or double integrators were studied in [13–16]. While for nonholonomic vehicles, several works studied the case where the target moves with a constant velocity. In particular, the authors in [17, 18] studied the case where the target is a vehicle and the linear velocities of all vehicles maintain constant. A Lyapunov guidance vector field approach was introduced in [19]. The authors also took into account the spaced formation of two vehicles and a target with an unknown constant velocity. Later, the spaced formation of multiple vehicles under a fixed sensor graph was further studied in [20]. If the velocity of the target is time-varying, it becomes more challenging to investigate the circular formation control problem even though its velocity is available to all vehicles [21]. It was shown in [21] that the tracking errors with respect to the circular motion around the target were locally uniformly bounded and did not converge to zero. In [22], a translation control design was developed such that global asymptotical stabilization of the circular formation can be achieved provided that measurements in the global inertial frame and communication among vehicles were available.

In this note, we consider a circular formation control problem similar to [22]. A static controller using only local measurements of each vehicle is proposed to achieve the evenly spaced circular formation of multiple vehicles around a moving-target. A cyclic pursuit strategy [14, 21] is used to generate the topology of the sensor graph which may dynamically switch based on the relative positions between vehicles and the target.

The main contributions of this work can be summarized into four aspects. First, the proposed controller only relies on local measurements in the Frenet-Serret frame of each vehicle. Thus, a global coordinate frame and communication among vehicles are not required, which makes the implementation easier in practice. Second, the tracking errors with respect to the circular motion around the target can globally converge to zero if the maximum velocity of the target is known and certain conditions on local measurements are satisfied. Third, the target does not have to be a vehicle of unicycle type and it is allowed to move with a time-varying velocity. Last but not least, the evenly spaced formation along the circle can be achieved and is reconfigurable when some vehicles are added into or removed from the fleet.

The rest of this note is organized as follows. In Section II, the problem formulation is introduced and two technical lemmas are reviewed. In Section III, we present the cooperative controller and establish stability of the closed-loop system. In Section IV, the simulation results of an example are shown, and in Section V the conclusion is drawn.

Notations: In the Cartesian coordinate plane, $\overrightarrow{\boldsymbol{ab}}$ denotes a vector from a point $\boldsymbol{a}$ to a point $\boldsymbol{b}$. $\|\boldsymbol{x}\|$ denotes the 2-norm of a vector $\boldsymbol{x} \in \mathbb{R}^n$, i.e., $\|\boldsymbol{x}\| = \sqrt{\sum_{i=1}^{n} |x_i|^2}$.

II. Preliminaries

A. Problem Formulation

Consider a fleet of N nonholonomic vehicles of unicycle type. The kinematics of each vehicle is described by:

$$\dot{x}_i = v_i \cos\theta_i,\ \dot{y}_i = v_i \sin\theta_i,\ \dot{\theta}_i = \omega_i,\ i = 1, 2, ..., N, \quad (1)$$

This work was supported by the Research Grants Council of the Hong Kong Special Administrative Region of China under Project CityU/11209514.

The authors are with Department of Mechanical and Biomedical Engineering, City University of Hong Kong, Kowloon, Hong Kong SAR, China. e-mail: xiaoyu4-c@my.cityu.edu.hk, luliu45@cityu.edu.hk.

where $\boldsymbol{p}_i := [x_i\ y_i]^{\mathrm{T}} \in \mathbb{R}^2$ is the absolute position and $\theta_i \in \mathbb{R}$ is the heading angle of each vehicle with respect to the inertial frame, $v_i \in \mathbb{R}$ and $\omega_i \in \mathbb{R}$ are its linear velocity and angular velocity respectively.

A target moves along a trajectory $\boldsymbol{c}(t) = [x_c(t)\ y_c(t)]^{\mathrm{T}}$, and the initial positions of the vehicles and the target satisfy the following assumption [13, 14, 21]:

[A1] All vehicles and the target are not co-located and have distinct locations at the initial time t_0, i.e., $\boldsymbol{p}_i(t_0) \neq \boldsymbol{p}_j(t_0) \neq \boldsymbol{c}(t_0),\ \forall i \neq j$.

As in [22], the trajectory $\boldsymbol{c}(t)$ is assumed to satisfy the following assumption:

[A2] $\boldsymbol{c}(t) : \mathbb{R}_{\geq 0} \to \mathbb{R}^2$ is a $\mathcal{C}^2$ function with bounded 1$^{\text{st}}$-order and 2$^{\text{nd}}$-order derivatives.

A moving-target circular formation requires all vehicles to travel along a common circle with the center $\boldsymbol{c}$ and a given radius r, and maintain even spacing along the circle.

Before presenting the formal definition of the problem, the neighboring strategy of the fleet of vehicles is first introduced. The strategy is adopted from [14] and [21], and is based on the positions of vehicles $\boldsymbol{p}_1$, ..., $\boldsymbol{p}_N$ in circular counter-clockwise radial order around the target $\boldsymbol{c}$. Define a node set $\mathcal{O} = \{1, 2, ..., N\}$ representing N vehicles. Let $\varphi_{ij} \in [0, 2\pi)$, $i,\ j \in \mathcal{O}$, be the *backward* separation angle by rotating the planar vector $\overrightarrow{\boldsymbol{c}\boldsymbol{p}_i}$ *clockwise* until its direction coinciding with that of $\overrightarrow{\boldsymbol{c}\boldsymbol{p}_j}$, and $\varphi_{ji} \in [0, 2\pi)$ be the *forward* separation angle by rotating $\overrightarrow{\boldsymbol{c}\boldsymbol{p}_i}$ *counterclockwise* until its direction coinciding with that of $\overrightarrow{\boldsymbol{c}\boldsymbol{p}_j}$. Then, let vehicle $i-$ satisfying $\|\boldsymbol{p}_{i-} - \boldsymbol{c}\| = \max_{j \in \mathcal{N}_i^{pre}} \|\boldsymbol{p}_j - \boldsymbol{c}\|$ be the *pre-neighbor* of vehicle i, and vehicle $i+$ satisfying $\|\boldsymbol{p}_{i+} - \boldsymbol{c}\| = \min_{j \in \mathcal{N}_i^{ne}} \|\boldsymbol{p}_j - \boldsymbol{c}\|$ be the *next-neighbor*, where $\mathcal{N}_i^{pre} = \{j \in \mathcal{O} | \varphi_{ij} = \min_{k \neq i} \varphi_{ik}\}$ and $\mathcal{N}_i^{ne} = \{j \in \mathcal{O} | \varphi_{ji} = \min_{k \neq i} \varphi_{ki}\}$. As an example show in Fig. 1(a), the counterclockwise radial order of vehicles is $1 \to 2 \to 5 \to 3 \to 4 \to 1$. Thus, the pre-neighbor and next-neighbor of vehicle 1 are vehicle 4 and vehicle 2 respectively. Based on this strategy, the IDs or labels of vehicles are not required. Each vehicle searches for its neighbors by sensing its counterclockwise and clockwise radial sides with respect to the target.

Denote $\boldsymbol{\varphi} = \mathrm{col}(\varphi_{(1+)1}, ..., \varphi_{(N+)N})$ and let $\mathcal{N}_i(\boldsymbol{\varphi})$ be the set including the neighbors of vehicle i. It follows from the neighboring strategy that $\mathcal{N}_i(\boldsymbol{\varphi}) = \{i+, i-\}$. Then, a state-dependent *sensor graph* $\mathcal{G}(\boldsymbol{\varphi}) = (\mathcal{O}, \mathcal{E}(\boldsymbol{\varphi}))$ with $\mathcal{E}(\boldsymbol{\varphi}) = \{(i, j) : j \in \mathcal{N}_i(\boldsymbol{\varphi}),\ i, j \in \mathcal{O}\}$ is used to describe the topology of the sensor network among vehicles. According to the neighboring strategy, although the edge set $\mathcal{E}(\boldsymbol{\varphi})$ may change as $\boldsymbol{\varphi}$ varies, the *sensor graph* $\mathcal{G}(\boldsymbol{\varphi})$ is a cycle if no vehicles are in the same position. Denote the Laplacian matrix of $\mathcal{G}(\boldsymbol{\varphi})$ by $\mathcal{L}(\boldsymbol{\varphi})$. When $\mathcal{G}(\boldsymbol{\varphi})$ is a cycle, $\mathcal{L}(\boldsymbol{\varphi})$ is positive semi-definite and satisfies $\mathcal{L}(\boldsymbol{\varphi})\mathbf{1}_N = \mathbf{1}_N^{\mathrm{T}}\mathcal{L}(\boldsymbol{\varphi}) = \mathbf{0}$.

In practice, neither absolute positions $\boldsymbol{p}_i$, $\boldsymbol{p}_j$, $\boldsymbol{c}$, nor relative positions $\boldsymbol{p}_i - \boldsymbol{c}$, $\boldsymbol{p}_i - \boldsymbol{p}_j$, $j \in \mathcal{N}_i(\boldsymbol{\varphi})$, can be measured due to the lack of a global coordinate frame or a common reference direction. As in [21], each vehicle i establishes its local coordinate frame, i.e., the Frenet-Serret frame, with the origin at its position $\boldsymbol{p}_i$ and the x-axis coincident with its heading angle θ_i. Then, the positions $\boldsymbol{c}$ and $\boldsymbol{p}_j$, $j \in \mathcal{N}_i(\boldsymbol{\varphi})$, measured in the global inertial frame can be converted to those in the local Frenet-Serret frame of vehicle i by using the following coordinate transformation [23]:

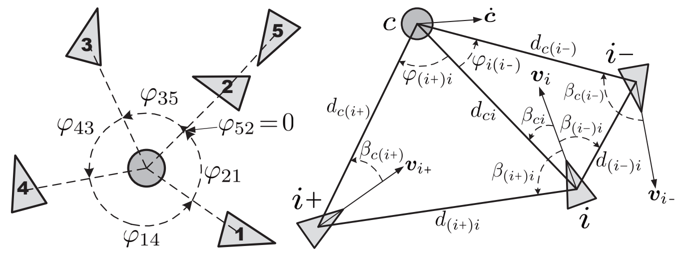

(a) Neighboring strategy (b) Local measurements

Fig. 1. Illustration of the neighboring strategy and measurements in the coordinate frame of vehicle i.

$$\boldsymbol{c}^i = [x_c^i\ y_c^i] = R(\theta_i)(\boldsymbol{c} - \boldsymbol{p}_i),\ \boldsymbol{p}_j^i = R(\theta_i)(\boldsymbol{p}_j - \boldsymbol{p}_i), \quad (2)$$

where $R(\theta_i) = \begin{bmatrix} \cos\theta_i & \sin\theta_i \\ -\sin\theta_i & \cos\theta_i \end{bmatrix}$. Besides, the real-time velocity and acceleration of the target measured in the local coordinate frame of vehicle i are

$$\boldsymbol{v}_c^i = R(\theta_i)\dot{\boldsymbol{c}},\ \boldsymbol{a}_c^i = R(\theta_i)\ddot{\boldsymbol{c}}, \quad (3)$$

respectively. As shown in Fig. 1(b), vehicle i can obtain $\boldsymbol{c}^i$ and $\boldsymbol{p}_j^i$ by measuring the relative distances d_{ci}, d_{ji} and bearing angles β_{ci}, β_{ji}, $j \in \mathcal{N}_i(\boldsymbol{\varphi})$. In fact, by sensing d_{ci}, d_{ji}, β_{ci} and β_{ji}, $j \in \mathcal{N}_i(\boldsymbol{\varphi})$, vehicle i can calculate $\varphi_{(i+)i}$ and $\varphi_{i(i-)}$ in the triangles $\triangle i(i+)c$ and $\triangle i(i-)c$ shown in Fig. 1(b) respectively.

Then, the following assumptions on local measurements are made:

[A3] Vehicle i can measure d_{ci}, β_{ci}, and the real-time velocity and acceleration of the target measured in local coordinate frame, i.e., $\boldsymbol{v}_c^i$ and $\boldsymbol{a}_c^i$. Besides, the constant $\sup\|\dot{\boldsymbol{c}}\|$ is known.

[A4] Vehicle i, $i \in \mathcal{O}$, can measure its own linear velocity v_i, relative distances d_{ji} and bearing angles β_{ji}, $j \in \mathcal{N}_i(\boldsymbol{\varphi})$.

Now, the formal definition of the *moving-target circular formation control problem* in this note is stated as follows.

Definition 2.1: Consider a target $\boldsymbol{c}(t)$ and a desired radius r. For vehicle i, $i = 1, ..., N$, with any initial state $[\boldsymbol{p}_i^{\mathrm{T}}(t_0)\ \theta_i(t_0)]^{\mathrm{T}} \in \mathbb{R}^3$, $\forall t_0 \geq 0$, design a controller $[\dot{v}_i\ \omega_i]^{\mathrm{T}}$ using the local measurements, i.e.,

$$[\dot{v}_i\ \omega_i]^{\mathrm{T}} = \boldsymbol{\varrho}(v_i, d_{ji}, \beta_{ji}, d_{ci}, \beta_{ci}, \boldsymbol{v}_c^i, \boldsymbol{a}_c^i),\ j \in \mathcal{N}_i(\boldsymbol{\varphi}), \quad (4)$$

such that the following objectives can be achieved:

(i) $\lim_{t\to\infty} (\boldsymbol{p}_i(t) - \boldsymbol{c}(t)) = r[\sin\phi_i(t)\ \ -\cos\phi_i(t)]^{\mathrm{T}}$, $r\dot{\phi}_i = u_c > 0$, $\forall i \in \mathcal{O}$, where ϕ_i is the vectorial angle of $\boldsymbol{v}_i - \dot{\boldsymbol{c}}$, i.e., $\phi_i = \angle(v_i\angle\theta_i - \dot{\boldsymbol{c}})$ (circular motion around the target);

(ii) $\lim_{t\to\infty} \|\boldsymbol{p}_i(t) - \boldsymbol{p}_{i+}(t)\| = \lim_{t\to\infty} \|\boldsymbol{p}_j(t) - \boldsymbol{p}_{j+}(t)\|$, $\forall i, j \in \mathcal{O}$, i.e., $\lim_{t\to\infty} \varphi_{(i+)i}(t) = 2\pi/N$, $\forall i \in \mathcal{O}$ (evenly spaced formation). ■

Remark 2.1: The assumptions that $\sup\|\dot{\boldsymbol{c}}\|$ is known and vehicle i can measure v_i in assumptions [A3]-[A4], as well as assumption [A2], are also required in [22]. Besides, in assumptions [A3]-[A4], vehicle i only uses its local coordinate frame instead of a global one. While in [22], vehicle i had access to $\dot{\boldsymbol{c}}$ and $\ddot{\boldsymbol{c}}$ measured in the global inertial frame, as well as the absolute position $\boldsymbol{p}_i$, $\boldsymbol{c}$, and the heading angle θ_i, which implies that vehicles had to share a global coordinate frame. Moreover, it was shown in [22] that vehicle i had to obtain some internal states of its neighbors, which implies that communication among vehicles must be used. While in assumption [A4], vehicle i only relies on local measurements and does not use any communication. ∎

B. Technical Lemmas

We now review two technical lemmas which will be used in the next section.

The first lemma introduced in [24] is often referred to as the so-called reduction theorem for asymptotic stability of sets, and the definition of relative set stability is given in Definition 4 in [24].

Lemma 2.1 (Proposition 14 in [24]): Consider a locally Lipschitz control system $\dot{\boldsymbol{\upsilon}} = \boldsymbol{f}(\boldsymbol{\upsilon}, \boldsymbol{\eta})$ with state space a domain $\Upsilon \in \mathbb{R}^q$, and assume that there exists a locally Lipschitz feedback $\bar{\boldsymbol{\eta}}(\boldsymbol{\upsilon})$ making the sets $\Gamma_n \subset \Gamma_{(n-1)} \subset \ldots \subset \Gamma_1$ positively invariant for the closed-loop system $\dot{\boldsymbol{\upsilon}} = \boldsymbol{f}(\boldsymbol{\upsilon}, \bar{\boldsymbol{\eta}}(\boldsymbol{\upsilon}))$. Let $\Gamma_0 := \Upsilon$, and if (i) For $i = 1, ..., n$, Γ_i is globally asymptotically stable relative to $\Gamma_{(i-1)}$ for the closed-loop system; (ii) All trajectories of the closed-loop system are bounded; (iii) Γ_n is compact, then Γ_n is globally asymptotically stable for the closed-loop system. ∎

Then, the second lemma is a version of the non-smooth LaSalle Invariance Principle given in [25].

Lemma 2.2 (Theorem 3.2, Chapter VII, [25]): Let $\boldsymbol{\upsilon}(t)$ be a solution of $\dot{\boldsymbol{\upsilon}} = \boldsymbol{f}(\boldsymbol{\upsilon})$, $\boldsymbol{\upsilon}(0) = \boldsymbol{\upsilon}_0 \in \mathbb{R}^q$, where $\boldsymbol{f} : \Upsilon \to \mathbb{R}^q$ is continuous with Υ an open subset of $\mathbb{R}^q$, and let $\mathcal{V} : \Upsilon \to \mathbb{R}$ be a locally Lipschitz function such that $\mathrm{D}^+\mathcal{V}(\boldsymbol{\upsilon}(t)) \le 0$, where D^+ is the upper right-hand derivative. With denoting the positive limit set of a solution $\boldsymbol{\upsilon}$ as $\Lambda^+(\boldsymbol{\upsilon})$, $\Lambda^+(\boldsymbol{\upsilon}) \bigcap \Upsilon$ is contained in the union of all solutions that remain in $\mathcal{S} = \{\boldsymbol{\upsilon} \in \Upsilon : \mathrm{D}^+\mathcal{V}(\boldsymbol{\upsilon}) = 0\}$. ∎

III. Main Results

In this section, first a cooperative controller is proposed to solve the *moving-target circular formation control problem*. Then, stability analysis of the closed-loop system consisting of the proposed controller and multi-vehicle system is provided.

A. Controller Design

Define the relative position between vehicle i and the target as

$$\tilde{\boldsymbol{p}}_i := [\tilde{x}_i \ \tilde{y}_i]^{\mathrm{T}} = \boldsymbol{p}_i - \boldsymbol{c}. \tag{5}$$

Then, under assumption [A2], the following error dynamics can be obtained by differentiating $\tilde{\boldsymbol{p}}_i$ with respect to time.

$$\dot{\tilde{x}}_i = u_i \cos\phi_i, \ \dot{\tilde{y}}_i = u_i \sin\phi_i, \ \dot{\phi}_i = \gamma_i, \tag{6}$$

where u_i and γ_i are respectively given as

$$u_i = (\dot{\tilde{x}}_i^2 + \dot{\tilde{y}}_i^2)^{\frac{1}{2}}, \ \gamma_i = (-\ddot{\tilde{x}}_i\dot{\tilde{y}}_i + \ddot{\tilde{y}}_i\dot{\tilde{x}}_i)/(\dot{\tilde{x}}_i^2 + \dot{\tilde{y}}_i^2). \tag{7}$$

As shown in [26], γ_i is derived from $\phi_i = \mathrm{atan2}(\dot{\tilde{y}}_i, \dot{\tilde{x}}_i)$ with the two-argument arctangent function $\mathrm{atan2}(\cdot) : \mathbb{R}^2 \setminus \{(0,0)\} \to [-\pi, \pi)$. System (6) models the dynamics of the planar vector $\boldsymbol{u}_i = u_i\angle\phi_i = [\dot{\tilde{x}}_i \ \dot{\tilde{y}}_i]^{\mathrm{T}}$, $u_i \neq 0$, obtained by the vector difference between $\boldsymbol{v}_i = v_i\angle\theta_i$ and $\dot{\boldsymbol{c}}$, i.e.,

$$\boldsymbol{u}_i = u_i\angle\phi_i = \boldsymbol{v}_i - \dot{\boldsymbol{c}}, \ u_i \neq 0. \tag{8}$$

Next, consider $[u_i \ \gamma_i]^{\mathrm{T}}$ as control input to the system in the form of (6). Use the local measurements to design controller $[\dot{v}_i \ \omega_i]^{\mathrm{T}}$ and relate it to $[u_i \ \gamma_i]^{\mathrm{T}}$, such that $\tilde{\boldsymbol{p}} := \mathrm{col}(\tilde{\boldsymbol{p}}_1^{\mathrm{T}}, ..., \tilde{\boldsymbol{p}}_N^{\mathrm{T}})$ converges to set $\Pi = \{\tilde{\boldsymbol{p}} \in \mathbb{R}^{2N} : \tilde{\boldsymbol{p}}_i = r[\sin\phi_i \ -\cos\phi_i]^{\mathrm{T}}, r\dot{\phi}_i = u_c, \varphi_{(i+)i}(\tilde{\boldsymbol{p}}) = 2\pi/N, \ i \in \mathcal{O}\}$, where $u_c > 0$ is some constant to be specified later.

Then, we propose the following controller for vehicle i, $i \in \mathcal{O}$.

$$\dot{v}_i = Q\boldsymbol{a}_c^i - k_1(u_i - \bar{u}_i)\cos\phi_i^i - u_i\bar{\gamma}_i\sin\phi_i^i, \tag{9}$$

$$\omega_i = \frac{u_i\bar{\gamma}_i + \dot{v}_i\sin\phi_i^i - [\sin\phi_i^i \ -\cos\phi_i^i]\boldsymbol{a}_c^i}{v_i\cos\phi_i^i}, \tag{10}$$

with

$$\bar{u}_i = u_c + k_2 r \sin\frac{1}{4}(\varphi_{(i+)i} - \varphi_{i(i-)}), \tag{11}$$

$$\bar{\gamma}_i = (u_i - k_3\sigma([\cos\phi_i^i \ \sin\phi_i^i]\boldsymbol{c}^i))/r, \tag{12}$$

where $Q = [1 \ \ 0]$, $k_1 > \frac{3}{4}k_2 > 0$, k_3 is any positive constant, u_c and k_2 are constants satisfying

$$u_c > \sup\|\dot{\boldsymbol{c}}\|, \ 0 < k_2 < (u_c - \sup\|\dot{\boldsymbol{c}}\|)/r. \tag{13}$$

Function $\sigma : \mathbb{R} \to \mathbb{R}$ is a $\mathcal{C}^1$ function such that (i) $\sigma(0) = 0$, (ii) $|\sigma(z)| \le 1$, $\forall z \in \mathbb{R}$, and (iii) $z\sigma(z) > 0$, $\forall z \in \mathbb{R}\backslash\{0\}$. For example, $\sigma(z) = \tanh(z)$ and $\sigma(z) = z/\sqrt{1+z^2}$. Moreover, ϕ_i^i is defined as

$$\phi_i^i = \phi_i - \theta_i, \tag{14}$$

which denotes the direction of $\boldsymbol{u}_i$ measured in the local coordinate frame of vehicle i, and ϕ_i^i can be calculated by

$$\cos\phi_i^i = (v_i^2 + u_i^2 - \|\dot{\boldsymbol{c}}\|^2)/(2v_iu_i). \tag{15}$$

Note that $\|\boldsymbol{v}_c^i\| = \|R(\theta_i)\dot{\boldsymbol{c}}\| = \|\dot{\boldsymbol{c}}\|$. Then, it follows from (3) and (8) that u_i can be calculated by

$$u_i = (v_i^2 + \|\boldsymbol{v}_c^i\|^2 - 2v_iQ\boldsymbol{v}_c^i)^{\frac{1}{2}}. \tag{16}$$

Thus, controller (9)-(10) with (11)-(12) is in the form of (4).

B. Main Theorem

Now, we state the main result as follows.

Theorem 3.1: Consider a target moving along a trajectory $\boldsymbol{c}(t)$ and N nonholonomic vehicles in the form of (1). Define u_i as in (16). If the initial condition $u_i(t_0) > \sup\|\dot{\boldsymbol{c}}\|$, $i = 1, ..., N$, is satisfied, controller (9)-(10) with (11)-(12) solves the *moving-target circular formation control problem* under assumptions [A1]-[A4]. ∎

Remark 3.1: The initial condition $u_i(t_0) > \sup\|\dot{\boldsymbol{c}}\|$ is a sufficient condition to exclude the occurrence of singular points $u_i = 0$ and $v_i \cos\phi_i^i = 0$ in (8) and (9), which will be shown later. In practice, $u_i(t_0) > \sup\|\dot{\boldsymbol{c}}\|$ can be enforced by

$$v_i(t_0) > 2\sup\|\dot{\boldsymbol{c}}\|. \tag{17}$$

Since $u_i = \|\boldsymbol{v}_i - \dot{\boldsymbol{c}}\|$ and $v_i(t_0) > 2\sup\|\dot{\boldsymbol{c}}\|$, the initial condition $u_i(t_0) > \sup\|\dot{\boldsymbol{c}}\|$ can be satisfied. It is noted that a common initial time is not required for the vehicles. Each vehicle i can "activate" the proposed controller individually at any instant t_0^i when $u_i(t_0^i) > \sup\|\dot{\boldsymbol{c}}\|$. ∎

In what follows, Theorem 3.1 will be proved by utilizing Lemma 2.1. First, the following three steps of set stabilization analysis will be given, and then Lemma 2.1 will be employed to arrive at Theorem 3.1. Denote $\boldsymbol{u} = \text{col}(u_1, ..., u_N)$ and define Γ_1 as

$$\Gamma_1 = \mathbb{R}^{2N} \times (\sup\|\dot{\boldsymbol{c}}\|, +\infty)^N.$$

Step 1: To show that Γ_1 is positively invariant for the closed-loop system, i.e., $[\tilde{\boldsymbol{p}}^{\mathrm{T}}(t)\ \boldsymbol{u}^{\mathrm{T}}(t)]^{\mathrm{T}} \in \Gamma_1$, $\forall t \geq t_0$ if $[\tilde{\boldsymbol{p}}^{\mathrm{T}}(t_0)\ \boldsymbol{u}^{\mathrm{T}}(t_0)]^{\mathrm{T}} \in \Gamma_1$.

Step 2: To stabilize set Γ_2 relative to set Γ_1, where

$$\Gamma_2 = \{[\tilde{\boldsymbol{p}}^{\mathrm{T}}\ \boldsymbol{u}^{\mathrm{T}}]^{\mathrm{T}} \in \Gamma_1 : \tilde{\boldsymbol{p}}_i = r\begin{bmatrix} \sin\phi_i \\ -\cos\phi_i \end{bmatrix}, u_i = r\dot{\phi}_i, i \in \mathcal{O}\}.$$

Step 3: To stabilize set Γ_3 relative to set Γ_2, where

$$\Gamma_3 = \{[\tilde{\boldsymbol{p}}^{\mathrm{T}}\ \boldsymbol{u}^{\mathrm{T}}]^{\mathrm{T}} \in \Gamma_2 : \varphi_{(i+)i}(\tilde{\boldsymbol{p}}) = 2\pi/N, u_i = u_c, i \in \mathcal{O}\}.$$

C. *Positive Invariance of* Γ_1

In the first step, we show that $[\tilde{\boldsymbol{p}}^{\mathrm{T}}(t)\ \boldsymbol{u}^{\mathrm{T}}(t)]^{\mathrm{T}} \in \Gamma_1$, $\forall t \geq t_0$ if $[\tilde{\boldsymbol{p}}^{\mathrm{T}}(t_0)\ \boldsymbol{u}^{\mathrm{T}}(t_0)]^{\mathrm{T}} \in \Gamma_1$, i.e., $\boldsymbol{u}(t) \geq \sup\|\dot{\boldsymbol{c}}\|$ if $\boldsymbol{u}(t_0) \geq \sup\|\dot{\boldsymbol{c}}\|$.

First, using (6), (14) and the following equations

$$\frac{d(u_i\cos\phi_i)}{dt}\cos\theta_i + \frac{d(u_i\sin\phi_i)}{dt}\sin\theta_i = \ddot{\tilde{x}}_i\cos\theta_i + \ddot{\tilde{y}}_i\sin\theta_i,$$

$$\ddot{\tilde{x}}_i = \dot{v}_i\cos\theta_i - v_i\omega_i\sin\theta_i - \ddot{x}_c, \tag{18}$$

$$\ddot{\tilde{y}}_i = \dot{v}_i\sin\theta_i + v_i\omega_i\cos\theta_i - \ddot{y}_c, \tag{19}$$

yields

$$\dot{u}_i\cos\phi_i^i = \dot{v}_i - (\ddot{x}_c\cos\theta_i + \ddot{y}_c\sin\theta_i) + \gamma_i u_i\sin\phi_i^i. \tag{20}$$

Noting that ϕ_i^i denotes the vectorial angle from $\boldsymbol{v}_i$ to $\boldsymbol{u}_i$, it follows from (8) that if $u_i > \|\dot{\boldsymbol{c}}\|$, then $v_i \neq 0$ and $\phi_i^i \in [0, \pi/2)$, i.e., $v_i\cos\phi_i^i \neq 0$. Thus, the singular points $u_i = 0$ and $v_i\cos\phi_i^i = 0$ can be avoided if $u_i > \|\dot{\boldsymbol{c}}\|$.

Next, supposing that $u_i(t) > \|\dot{\boldsymbol{c}}(t)\|$ holds, and using (6)-(7) yield

$$\gamma_i = (\ddot{\tilde{y}}_i\cos\phi_i - \ddot{\tilde{x}}_i\sin\phi_i)/u_i. \tag{21}$$

Substituting (18) and (19) into (21) leads to

$$\gamma_i = \frac{\ddot{x}_c\sin\phi_i - \ddot{y}_c\cos\phi_i - \dot{v}_i\sin\phi_i^i + v_i\omega_i\cos\phi_i^i}{u_i}, \tag{22}$$

and then substituting (10) into (22) gives

$$\gamma_i = \bar{\gamma}_i. \tag{23}$$

Moreover, if $u_i(t) > \|\dot{\boldsymbol{c}}(t)\|$ holds, using $Q\boldsymbol{a}_c^i = \ddot{x}_c\cos\theta_i + \ddot{y}_c\sin\theta_i$, and substituting (9) and (23) into (20) yield

$$\dot{u}_i = \frac{\dot{v}_i - Q\boldsymbol{a}_c^i + \bar{\gamma}_i u_i\sin\phi_i^i}{\cos\phi_i^i} = -k_1 u_i + k_1\bar{u}_i. \tag{24}$$

Now, we claim that if the initial condition $u_i(t_0) > \sup\|\dot{\boldsymbol{c}}\|$ is satisfied, then $u_i(t) > \sup\|\dot{\boldsymbol{c}}\|$ holds for all $t \geq t_0$.

We prove the claim by contradiction. By assumption [A2] and (16), $u_i(t)$ is differentiable in t. Since $u_i(t_0) > \sup\|\dot{\boldsymbol{c}}\|$, if the claim is not true, there must exist an instant $t_u > t_0$ such that $u_i(t_u) = \sup\|\dot{\boldsymbol{c}}\|$ and $u_i(t) > \sup\|\dot{\boldsymbol{c}}\|$ for $t_0 \leq t < t_u$. Then, it follows from (24) that for all $0 \leq t < t_u$,

$$u_i(t) = e^{-k_1(t-t_0)}u_i(t_0) + \int_{t_0}^{t} e^{-k_1(t-\tau)}k_1\bar{u}_i(\tau)d\tau. \tag{25}$$

Using (11) and (13), we have $\bar{u}_i \geq u_c - k_2 r \geq \sup\|\dot{\boldsymbol{c}}\|$. Then, it follows that for all $0 \leq t < t_u$,

$$\begin{aligned} u_i(t) &\geq e^{-k_1(t-t_0)}u_i(t_0) + k_1(u_c - k_2 r)\int_{t_0}^{t} e^{-k_1(t-\tau)}d\tau \\ &= e^{-k_1(t-t_0)}u_i(t_0) + \sup\|\dot{\boldsymbol{c}}\|(1 - e^{-k_1(t-t_0)}) \\ &\geq e^{-k_1(t-t_0)}(u_i(t_0) - \sup\|\dot{\boldsymbol{c}}\|) + \sup\|\dot{\boldsymbol{c}}\|. \end{aligned} \tag{26}$$

Since $u_i(t_0) - \sup\|\dot{\boldsymbol{c}}\| > 0$, then the left-hand limit $\lim_{t\to t_u^-} u_i(t) > \sup\|\dot{\boldsymbol{c}}\|$. Noting that $u_i(t)$ is differentiable in t, we have $u_i(t_u) = \lim_{t\to t_u^-} u_i(t) > \sup\|\dot{\boldsymbol{c}}\|$, which contradicts $u_i(t_u) = \sup\|\dot{\boldsymbol{c}}\|$. This proves the claim.

Hence, we can conclude that $u_i(t) > \|\dot{\boldsymbol{c}}\|$ holds for all $t \geq t_0$ if $u_i(t_0) > \sup\|\dot{\boldsymbol{c}}\|$. Then, the singular points $u_i = 0$ and $v_i\cos\phi_i^i = 0$ can be avoided for all $t \geq t_0$, and (24) also holds for all $t \geq t_0$. Since $\bar{u}_i \leq u_c + k_2 r$, we have

$$\begin{aligned} u_i(t) &\leq e^{-k_1(t-t_0)}u_i(t_0) + k_1(u_c + k_2 r)\int_{t_0}^{t} e^{-k_1(t-\tau)}d\tau \\ &= e^{-k_1(t-t_0)}u_i(t_0) + (u_c + k_2 r)(1 - e^{-k_1(t-t_0)}) \\ &\leq u_i(t_0) + u_c + k_2 r, \qquad \forall t \geq t_0. \end{aligned} \tag{27}$$

Thus, $u_i(t)$ is uniformly bounded. In turn, $[\dot{\tilde{x}}_i\ \dot{\tilde{y}}_i]^{\mathrm{T}}$ is bounded and $\tilde{\boldsymbol{p}}_i(t)$ is well-defined for all $t \geq t_0$ in the sense that the possibility of finite escape times is excluded.

All these arguments are summarized in the following proposition.

Proposition 3.1: Consider N systems in the form of (6) and (20) under assumptions [A2]-[A4]. If $u_i(t_0) > \sup\|\dot{\boldsymbol{c}}\|$, $i \in \mathcal{O}$, controllers (9)-(10) with (11)-(12) guarantee that Γ_1 is positively invariant for the closed-loop system, and $u_i \neq 0$ and $v_i\cos\phi_i^i \neq 0$ hold for all $[\tilde{\boldsymbol{p}}^{\mathrm{T}}\ \boldsymbol{u}^{\mathrm{T}}]^{\mathrm{T}} \in \Gamma_1$. Moreover, $\boldsymbol{u}$ is uniformly bounded and $\tilde{\boldsymbol{p}}$ is globally well-defined. ∎

D. *Asymptotic Stabilization of* Γ_2 *Relative to* Γ_1

In the second step, we show that all vehicles can converge to a circular motion around the moving-target with radius r. i.e., prove that $\tilde{\boldsymbol{p}}_i$ converge to $r[\sin\phi_i\ -\cos\phi_i]^{\mathrm{T}}$. To this end, define the tracking error $\bar{\boldsymbol{p}}_i := [\bar{x}_i\ \bar{y}_i]^{\mathrm{T}}$ as

$$\bar{x}_i = \tilde{x}_i - r\sin\phi_i,\ \bar{y}_i = \tilde{y}_i + r\cos\phi_i. \tag{28}$$

Consider a Lyapunov function candidate $V_i(\bar{\boldsymbol{p}}_i) = \frac{1}{2}\bar{\boldsymbol{p}}_i^{\mathrm{T}}\bar{\boldsymbol{p}}_i$. Taking the time derivative of $V_i(\bar{\boldsymbol{p}}_i)$ along system (6) yields

$$\dot{V}_i(\bar{\boldsymbol{p}}_i) = (\bar{x}_i \cos\phi_i + \bar{y}_i \sin\phi_i)(u_i - r\gamma_i). \tag{29}$$

Using Proposition 3.1, $u_i > \sup\|\dot{\boldsymbol{c}}\|$ and $v_i \cos\phi_i^i \neq 0$ for all $[\tilde{\boldsymbol{p}}^{\mathrm{T}}\ \boldsymbol{u}^{\mathrm{T}}]^{\mathrm{T}} \in \Gamma_1$, and then (23) holds for all $t \geq t_0$. Define

$$\Delta_i = \bar{x}_i \cos\phi_i + \bar{y}_i \sin\phi_i. \tag{30}$$

Substituting (12) and (23) into (29), using

$$-[\cos\phi_i^i\ \ \sin\phi_i^i]\boldsymbol{c}^i = \bar{x}_i \cos\phi_i + \bar{y}_i \sin\phi_i = \Delta_i, \tag{31}$$

and recalling the property (iii) of function $\sigma(\cdot)$ lead to

$$\dot{V}_i(\bar{\boldsymbol{p}}_i) = -k_3\Delta_i\sigma(\Delta_i) \leq 0. \tag{32}$$

Define $S_i = \{\bar{\boldsymbol{p}}_i \in \mathbb{R}^2 : \dot{V}_i(\bar{\boldsymbol{p}}_i) = 0\}$. From Proposition 3.1 and (28), $\bar{\boldsymbol{p}}_i(t)$ is well-defined for all $t \geq t_0$. This fact and the fact that $\dot{V}_i(\bar{\boldsymbol{p}}_i) \leq 0$ imply that S_i is globally stable. By (32), we have $S_i = \{\bar{\boldsymbol{p}}_i \in \mathbb{R}^2 : \Delta_i = 0\}$. When $\Delta_i = 0$, it follows from $\dot{\phi}_i = \gamma_i$, (12), (23), and (31) that $\dot{\phi}_i = u_i/r > \sup\|\dot{\boldsymbol{c}}\|/r$ and then ϕ_i is time-varying. Thus, set $\{\bar{\boldsymbol{p}}_i \in \mathbb{R}^2 : \bar{\boldsymbol{p}}_i \neq \boldsymbol{0},\ \Delta_i = 0\}$ is an unstable equilibrium set, and we have $S_i = \{\bar{\boldsymbol{p}}_i \in \mathbb{R}^2 : \bar{\boldsymbol{p}}_i = \boldsymbol{0}\}$. By LaSalle's Invariance Principle, every trajectory $\bar{\boldsymbol{p}}_i(t)$ approaches S_i as $t \to \infty$, i.e., every $\tilde{\boldsymbol{p}}_i(t)$ converges to $r[\sin\phi_i(t)\ -\cos\phi_i(t)]^{\mathrm{T}}$ for any $\tilde{\boldsymbol{p}}_i(t_0) \in \mathbb{R}^2$. Thus, $\tilde{\boldsymbol{p}}(t)$ is globally uniformly bounded and Γ_2 is globally asymptotically stable relative to Γ_1.

All these arguments are summarized in the following proposition.

Proposition 3.2: Consider N systems in the form of (6) and (20) under assumptions [A2]-[A4]. Controllers (9)-(10) with (11)-(12) guarantee that $\tilde{\boldsymbol{p}}(t)$ is globally uniformly bounded, and Γ_2 is globally asymptotically stable relative to Γ_1. ■

Remark 3.2: Although topology switchings of $\mathcal{G}(\boldsymbol{\varphi})$ may occur when $\varphi_{(i+)i} = 0$, $\forall i \in \mathcal{O}$, it follows from Propositions 3.1 and 3.2 that each vehicle converges to the circular motion around the target independent of the topology of $\mathcal{G}(\boldsymbol{\varphi})$. ■

E. Asymptotic Stabilization of Γ_3 Relative to Γ_2

In the third step, we show that vehicles which are orbiting around the target can maintain evenly spaced.

According to the neighboring strategy, for vehicles traveling along a common circle, the sensor graph $\mathcal{G}(\boldsymbol{\varphi})$ is a cycle unless it is at a switching instant, i.e., an instant t_s when $\varphi_{(i+)i}(t_s) = 0$, $\forall i \in \mathcal{O}$. The cycle $\mathcal{G}(\boldsymbol{\varphi})$ will remain to be degenerate if there exist at least two synchronized vehicles traveling on the circle. In this case, we can show that all the vehicles are synchronized as follows.

Suppose that the vehicles under assumption [A1] converge to set Γ_2 in which two neighboring vehicles k and $k+$ are synchronized, i.e., $\varphi_{(k+)k} = 0$, $\phi_k = \phi_{k+}$, and $\dot{\phi}_k = \dot{\phi}_{k+}$. Since $\dot{\phi}_i = u_i/r$, $\forall i \in \mathcal{O}$, then $u_k = u_{k+}$ and $\dot{u}_k = \dot{u}_{k+}$. By (24), we have $\bar{u}_k = \bar{u}_{k+}$. Then, it follows from (11) that $\sin\frac{1}{4}(0 - \varphi_{k(k-)}) = \sin\frac{1}{4}(\varphi_{(k++)k+} - 0)$. Since $\sin\frac{z}{4}$ is monotonous if $z \in [0, 2\pi)$ and $\varphi_{(i+)i} \in [0, 2\pi)$, for all $i \in \mathcal{O}$, then $\sin\frac{1}{4}(-\varphi_{k(k-)}) = \sin\frac{1}{4}(\varphi_{(k++)k+}) = 0$ and $\varphi_{k(k-)} = \varphi_{(k++)k+} = 0$. By induction, $\varphi_{(i+)i} = 0$, $\forall i \in \mathcal{O}$, which implies that all the vehicles are synchronized.

This scenario occurs if all the vehicles start with the same state (N vehicles reduce to one vehicle) or all the vehicles achieve synchronization under the proposed controllers. However, the vehicles are not initially co-located under assumption [A1], and as analyzed below, the proposed controllers (9)-(10) with (11)-(12) make vehicles approach separation instead of synchronization. Therefore, it can be concluded that the cycle will not remain to be degenerate unless the vehicles are synchronized already.

Since vehicles are traveling along a circle, i.e., $[\tilde{\boldsymbol{p}}^{\mathrm{T}}\ \boldsymbol{u}^{\mathrm{T}}]^{\mathrm{T}} \in \Gamma_2$, each separation angle $\varphi_{(i+)i}$ can be calculated by

$$\varphi_{(i+)i} = \phi_{i+} - \phi_i + \varepsilon_i, \tag{33}$$

where ε_i is defined as $\varepsilon_i = 2\pi$ if $\phi_{i+} - \phi_i < 0$, otherwise $\varepsilon_i = 0$. If all vehicles are dispersed on the circle, there is only one ε_i equal to 2π and all others are 0. Then, we further define

$$\chi_i = \varphi_{(i+)i} - \varphi_{i(i-)}, \tag{34}$$

and thus $\chi_i \in (-2\pi, 2\pi)$. By denoting $\boldsymbol{\chi} = \mathrm{col}(\chi_1, ..., \chi_N)$ and $\boldsymbol{\phi} = \mathrm{col}(\phi_1, ..., \phi_N)$, we have $\boldsymbol{\chi} = -\mathcal{L}(\boldsymbol{\varphi})\boldsymbol{\phi} + \boldsymbol{\zeta}$, where $\mathcal{L}(\boldsymbol{\varphi})$ is Laplacian matrix of $\mathcal{G}(\boldsymbol{\varphi})$ and $\boldsymbol{\zeta} = \mathrm{col}(\zeta_1, ..., \zeta_N)$ with $\zeta_i = \varepsilon_i - \varepsilon_{i-}$. Moreover, define a function $\boldsymbol{s}(\boldsymbol{z}) : \mathbb{R}^N \to [-1, 1]^N$ as

$$\boldsymbol{s}(\boldsymbol{z}) = \mathrm{col}(\sin\frac{z_1}{4}, ..., \sin\frac{z_N}{4}), \tag{35}$$

where z_i is the i^{th} entry of $\boldsymbol{z}$. Note that $\boldsymbol{s}(\boldsymbol{z})$ is monotonous if $\boldsymbol{z} \in (-2\pi, 2\pi)^N$, and $\boldsymbol{s}(\boldsymbol{0}) = \boldsymbol{0}$ if $\boldsymbol{z} = \boldsymbol{0}$. Denote $\bar{\boldsymbol{u}} = \mathrm{col}(\bar{u}_1, .., \bar{u}_N)$, and it follows from (11) that $\bar{\boldsymbol{u}} = u_c\boldsymbol{1}_N + k_2 r\boldsymbol{s}(-\mathcal{L}(\boldsymbol{\varphi})\boldsymbol{\phi} + \boldsymbol{\zeta})$.

Next, define $\Upsilon = [-\pi, \pi)^N \times (\sup\|\dot{\boldsymbol{c}}\|, +\infty)^N$ and consider a locally Lipschitz function $\mathcal{V}(\boldsymbol{\phi}, \boldsymbol{u}) : \Upsilon \to \mathbb{R}$ as

$$\begin{aligned}\mathcal{V} = {} & 2(\boldsymbol{u} - \bar{\boldsymbol{u}}(-\mathcal{L}(\boldsymbol{\varphi})\boldsymbol{\phi} + \boldsymbol{\zeta}))^{\mathrm{T}}\mathcal{L}(\boldsymbol{\varphi})(\boldsymbol{u} - \bar{\boldsymbol{u}}(-\mathcal{L}(\boldsymbol{\varphi})\boldsymbol{\phi} + \boldsymbol{\zeta})) \\ & + 2k_2^2 r^2 \boldsymbol{s}^{\mathrm{T}}(-\mathcal{L}(\boldsymbol{\varphi})\boldsymbol{\phi} + \boldsymbol{\zeta})\mathcal{L}(\boldsymbol{\varphi})\boldsymbol{s}(-\mathcal{L}(\boldsymbol{\varphi})\boldsymbol{\phi} + \boldsymbol{\zeta}).\end{aligned} \tag{36}$$

Since the topology of the sensor graph $\mathcal{G}(\boldsymbol{\varphi})$ may switch, $\mathcal{V}(\boldsymbol{\phi}, \boldsymbol{u})$ is not continuously differentiable at the switching instants if there is any. However, the topology of $\mathcal{G}(\boldsymbol{\varphi})$ remains unchanged when not at the switching instants, and $\mathcal{V}(\boldsymbol{\phi}, \boldsymbol{u})$ is piecewise continuously differentiable along the solutions of N systems (24) and $\dot{\phi}_i = u_i/r$.

Motivated by [14], the upper right-hand time derivative of $\mathcal{V}$, i.e., $\mathrm{D}^+\mathcal{V}$ is used for analysis. Since $\mathcal{G}(\boldsymbol{\varphi})$ is a cycle when it is not at the switching instants if there is any, $\mathcal{L}(\boldsymbol{\varphi}) = \mathcal{L}^{\mathrm{T}}(\boldsymbol{\varphi})$ and $\mathcal{L}(\boldsymbol{\varphi})\bar{\boldsymbol{u}} = k_2 r\mathcal{L}(\boldsymbol{\varphi})\boldsymbol{s}(\boldsymbol{\chi})$. By using $\boldsymbol{\chi} = -\mathcal{L}(\boldsymbol{\varphi})\boldsymbol{\phi} + \boldsymbol{\zeta}$, $\dot{\boldsymbol{\phi}} = \bar{\boldsymbol{u}}/r + (\boldsymbol{u} - \bar{\boldsymbol{u}})/r$, $\dot{\boldsymbol{u}} = -k_1(\boldsymbol{u} - \bar{\boldsymbol{u}})$, and $\bar{\boldsymbol{u}} = u_c\boldsymbol{1}_N + k_2 r\boldsymbol{s}(\boldsymbol{\chi})$, and denoting $\check{\boldsymbol{u}} = \boldsymbol{u} - \bar{\boldsymbol{u}}$ and $W(\boldsymbol{\chi}) = \mathrm{diag}(\cos\frac{\chi_1}{4}, ..., \cos\frac{\chi_N}{4})$, we obtain

$$\begin{aligned}\mathrm{D}^+\mathcal{V} = {} & 4\check{\boldsymbol{u}}^{\mathrm{T}}\mathcal{L}(\boldsymbol{\varphi})(-k_1\check{\boldsymbol{u}} - \mathrm{D}^+\bar{\boldsymbol{u}}) - k_2^2 r\boldsymbol{s}^{\mathrm{T}}(\boldsymbol{\chi})\mathcal{L}(\boldsymbol{\varphi})W(\boldsymbol{\chi})\mathcal{L}(\boldsymbol{\varphi})\check{\boldsymbol{u}} \\ & - k_2^3 r^2\boldsymbol{s}^{\mathrm{T}}(\boldsymbol{\chi})\mathcal{L}(\boldsymbol{\varphi})W(\boldsymbol{\chi})\mathcal{L}(\boldsymbol{\varphi})\boldsymbol{s}(\boldsymbol{\chi}) \\ = {} & -4k_1\check{\boldsymbol{u}}^{\mathrm{T}}\mathcal{L}(\boldsymbol{\varphi})\check{\boldsymbol{u}} + k_2\check{\boldsymbol{u}}^{\mathrm{T}}\mathcal{L}(\boldsymbol{\varphi})W(\boldsymbol{\chi})\mathcal{L}(\boldsymbol{\varphi})\check{\boldsymbol{u}} \\ & + k_2\check{\boldsymbol{u}}^{\mathrm{T}}\mathcal{L}(\boldsymbol{\varphi})W(\boldsymbol{\chi})\mathcal{L}(\boldsymbol{\varphi})\bar{\boldsymbol{u}} - k_2^2 r\boldsymbol{s}^{\mathrm{T}}(\boldsymbol{\chi})\mathcal{L}(\boldsymbol{\varphi})W(\boldsymbol{\chi})\mathcal{L}(\boldsymbol{\varphi})\check{\boldsymbol{u}} \\ & - k_2^3 r^2\boldsymbol{s}^{\mathrm{T}}(\boldsymbol{\chi})\mathcal{L}(\boldsymbol{\varphi})W(\boldsymbol{\chi})\mathcal{L}(\boldsymbol{\varphi})\boldsymbol{s}(\boldsymbol{\chi}) \\ = {} & -(\boldsymbol{u} - \bar{\boldsymbol{u}})^{\mathrm{T}}(4k_1\mathcal{L}(\boldsymbol{\varphi}) - k_2\mathcal{L}(\boldsymbol{\varphi})W(\boldsymbol{\chi})\mathcal{L}(\boldsymbol{\varphi}))(\boldsymbol{u} - \bar{\boldsymbol{u}}) \\ & - k_2^3 r^2\boldsymbol{s}^{\mathrm{T}}(\boldsymbol{\chi})\mathcal{L}(\boldsymbol{\varphi})W(\boldsymbol{\chi})\mathcal{L}(\boldsymbol{\varphi})\boldsymbol{s}(\boldsymbol{\chi}).\end{aligned} \tag{37}$$

Since $\chi_i \in (-2\pi, 2\pi)$, then $\cos\frac{\chi_1}{4} \in (0, 1]$ and the diagonal matrix $W(\boldsymbol{\chi})$ is always positive definite. Noting that $\mathcal{L}(\boldsymbol{\varphi})$ is the Laplacian matrix of a cycle, $k_1 > \frac{3}{4}k_2$, and $\cos\frac{\chi_1}{4} \in (0, 1]$, $4k_1\mathcal{L}(\boldsymbol{\varphi}) - k_2\mathcal{L}(\boldsymbol{\varphi})W(\boldsymbol{\chi})\mathcal{L}(\boldsymbol{\varphi})$ is a symmetric and weak diagonally dominant matrix with all diagonal elements positive. Thus, we have

$$\mathrm{D}^+\mathcal{V} \leq 0. \tag{38}$$

Define $\mathcal{S} = \{[\boldsymbol{\phi}^{\mathrm{T}}\ \boldsymbol{u}^{\mathrm{T}}]^{\mathrm{T}} \in \Upsilon : \mathrm{D}^+\mathcal{V} = 0\}$. It follows from (11), (37), and $\mathcal{L}(\boldsymbol{\varphi})\mathbf{1}_N = \mathbf{0}$ that $\mathcal{S} = \{[\boldsymbol{\phi}^{\mathrm{T}}\ \boldsymbol{u}^{\mathrm{T}}]^{\mathrm{T}} \in \Upsilon : \boldsymbol{\chi} = -\mathcal{L}(\boldsymbol{\varphi})\boldsymbol{\phi} + \boldsymbol{\zeta}, \sin\frac{\chi_i}{4} = \sin\frac{\chi_j}{4}, \forall i, j \in \mathcal{O}\}$. Using (34) yields $\sum_{i=1}^{N}\chi_i \equiv 0$, which together with $\chi_i \in (-2\pi, 2\pi)$, $\forall i \in \mathcal{O}$, implies $\mathcal{S} = \{[\boldsymbol{\phi}^{\mathrm{T}}\ \boldsymbol{u}^{\mathrm{T}}]^{\mathrm{T}} \in \Upsilon : -\mathcal{L}(\boldsymbol{\varphi})\boldsymbol{\phi} + \boldsymbol{\zeta} = \mathbf{0}_N\}$ and $\bar{\boldsymbol{u}} = u_c\mathbf{1}_N$ by (11). According to (24) and $\bar{\boldsymbol{u}} = u_c\mathbf{1}_N$, $\mathcal{S} = \{[\boldsymbol{\phi}^{\mathrm{T}}\ \boldsymbol{u}^{\mathrm{T}}]^{\mathrm{T}} \in \Upsilon : -\mathcal{L}(\boldsymbol{\varphi})\boldsymbol{\phi} + \boldsymbol{\zeta} = \mathbf{0}_N, \boldsymbol{u} = u_c\mathbf{1}_N\}$. By Lemma 2.2, $[\boldsymbol{\phi}^{\mathrm{T}}(t)\ \boldsymbol{u}^{\mathrm{T}}(t)]^{\mathrm{T}}$ approaches $\mathcal{S}$, i.e., $\boldsymbol{\chi}(t) \to \mathbf{0}_N$ and $\boldsymbol{u}(t) \to u_c\mathbf{1}_N$ as $t \to \infty$. It follows from (34) that $\lim_{t\to\infty}\varphi_{(i+)i}(t) = \lim_{t\to\infty}\varphi_{(j+)j}(t)$, $\forall i, j \in \mathcal{O}$. By (33), $\sum_{i=1}^{N}\varphi_{(i+)i} \equiv 2\pi$ and then $\lim_{t\to\infty}\varphi_{(i+)i}(t) = 2\pi/N$, $\forall i \in \mathcal{O}$. Thus, Γ_3 is globally asymptotically stable relative to Γ_2.

The above analysis is summarized in the following proposition.

Proposition 3.3: Consider N systems in the form of (6) and (20) under assumptions [A1]-[A4]. Controllers (9) with (11) make Γ_3 globally asymptotically stable relative to Γ_2. ∎

Remark 3.3: The topology of $\mathcal{G}(\boldsymbol{\varphi})$ may switch as $\boldsymbol{\varphi}$ varies, and switching only occurs when $\varphi_{(i+)i} = 0$, $\forall i \in \mathcal{O}$. As in [14], the upper right-hand time derivative of the Lyapunov function candidate is used for stability analysis in this case. When $[\tilde{\boldsymbol{p}}^{\mathrm{T}}\ \boldsymbol{u}^{\mathrm{T}}]^{\mathrm{T}}$ enters a small neighborhood of Γ_3, the topology of $\mathcal{G}(\boldsymbol{\varphi})$ will not switch. ∎

F. Proof of Theorem 3.1

Now, we are ready to prove Theorem 3.1 as follows.

Proof: Note that $\Gamma_3 \subset \Gamma_2 \subset \Gamma_1$. By Propositions 3.1, Γ_1 is positively invariant for the closed-loop system, which together with Propositions 3.2 and 3.3 implies that condition (i) of Lemma 2.1 is satisfied under assumptions [A1]-[A4]. Propositions 3.1 and 3.2 also imply that $[\tilde{\boldsymbol{p}}^{\mathrm{T}}\ \boldsymbol{u}^{\mathrm{T}}]^{\mathrm{T}}$ is uniformly bounded and thus condition (ii) of Lemma 2.1 is also satisfied. Since Γ_3 is compact, Lemma 2.1 indicates that Γ_3 is globally asymptotically stable relative to Γ_1 under assumptions [A1]-[A4]. Theorem 3.1 is thus proved. ∎

Remark 3.4: Similar to [22], each vehicle needs to have access to the motion of the target, which requires that the sensor range is sufficiently large or the motion of the target is a priori given. Moreover, in order to sense the neighboring vehicles, the sensor range of each vehicle needs to be larger than $2r\sin\frac{\pi}{N}$. Similar to the analysis in [22], the sensor graph $\mathcal{G}(\boldsymbol{\varphi})$ can become a cycle when all vehicles converge to the circular motion around the target. ∎

Remark 3.5: From a practical view of point, it is not easy to measure the velocity and acceleration of the target. If they are not a priori known to the vehicles, each vehicle is required to be equipped with a speedometer and an accelerometer. For example, a low-cost small-sized solid-state accelerometer described in [27] can be used to measure the acceleration. ∎

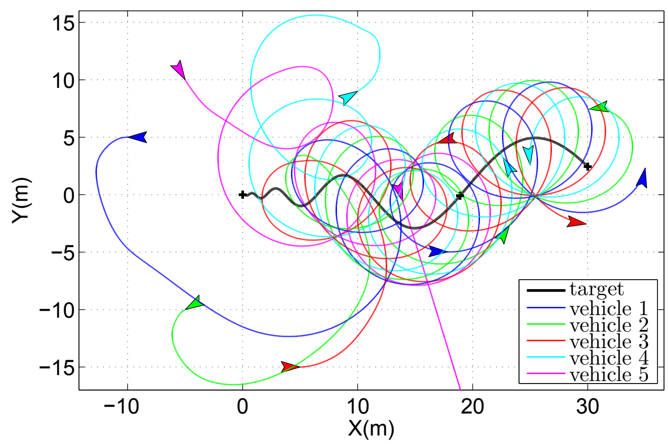

Fig. 2. Trajectories of all vehicles and the target during 0-180s.

Remark 3.6: In [17, 18], it was assumed that the target is also a unicycle-type vehicle and all vehicles have *constant* linear velocities. In [19] and [20], the velocity of the target $\dot{\boldsymbol{c}}(t)$ was assumed to be an unknown *constant* vector. While we consider the case where the target moves along any trajectory satisfying assumption [A2] with a time-varying velocity. ∎

Remark 3.7: The objective for a spaced formation was not included in [17, 18]. The spaced formation of two vehicles and multiple vehicles under a *fixed* sensor graph was achieved in [19] and [20] respectively. While with our proposed controller, an evenly spaced formation is achieved and can be reconfigurable as in [21] when some vehicles are added into or removed from the fleet. ∎

Remark 3.8: It is shown in [21] that the tracking errors with respect to circular motion around the target were locally uniformly bounded and did not converge to zero. While with our proposed controller, the tracking errors can globally converge to zero if assumptions [A2]-[A4] are satisfied. As stated in Remark 2.1, assumptions [A3]-[A4] are less restrictive than those in [22]. Compared with [22], our proposed controller can be applied to the case where neither a global coordinate frame nor communication among vehicles is available. ∎

IV. An Illustrative Example

Consider a fleet of 5 nonholonomic vehicles (1) and a target in a 2-D plane. The target $\boldsymbol{c}(t)$ and the desired radius r are given by $\boldsymbol{c}(t) = [0.3t\ \ 0.06t\sin(6\ln(t{+}1))]^{\mathrm{T}}$ and $r = 5$ respectively. The initial states of the vehicles are $\boldsymbol{p}_1(0) = [-10\ 5]^{\mathrm{T}}$, $\boldsymbol{p}_2(0) = [-5\ \ -10]^{\mathrm{T}}$, $\boldsymbol{p}_3(0) = [5\ \ -15]^{\mathrm{T}}$, $\boldsymbol{p}_4(0) = [10\ 9]^{\mathrm{T}}$, $\boldsymbol{p}_5(0) = [-5\ 10]^{\mathrm{T}}$, $\theta_1(0) = \pi$, $\theta_2(0) = -5\pi/6$, $\theta_3(0) = 0$, $\theta_4(0) = \pi/6$, and $\theta_5(0) = -\pi/3$. The initial linear velocities of the vehicles are $v_1(0) = 1.5$, $v_2(0) = 1$, $v_3(0) = 3$, $v_4(0) = 2$, and $v_5(0) = 2.5$, which satisfies (17). Thus, the initial condition $u_i > \sup\|\dot{\boldsymbol{c}}\|$ is met. Set $\sigma(\cdot) = \tanh(\cdot)$ and choose the parameters as $u_c = 2$, $k_1 = 1$, $k_2 = 0.6$ and $k_3 = 1$.

Suppose that vehicle 5 leaves the fleet at the instant $t_c = 63$s. Fig. 2 presents the trajectories of the target and all vehicles during $0-100$s. During $0-t_c$, all controlled vehicles converge to an evenly spaced circular formation around the

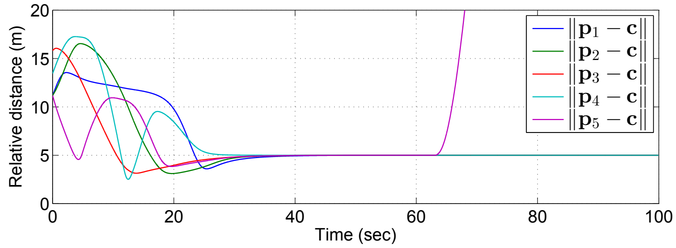

Fig. 3. Relative distance $\|\boldsymbol{p}_i(t) - \boldsymbol{c}(t)\|$.

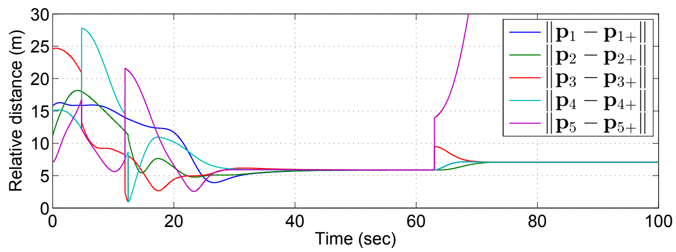

Fig. 4. Relative distance $\|\boldsymbol{p}_i(t) - \boldsymbol{p}_{i+}(t)\|$.

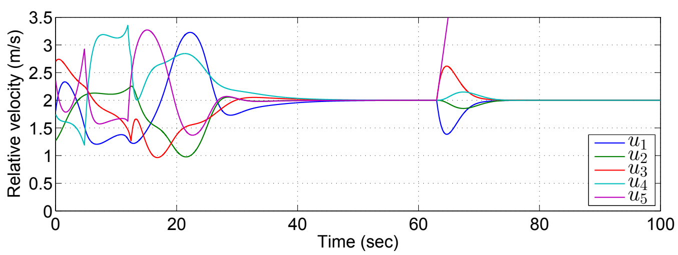

Fig. 5. Relative velocity $u_i(t)$.

target. When vehicle 5 leaves the fleet at t_c, the remaining 4 vehicles adaptively reconfigure themselves and resume evenly spaced again. Fig. 3 shows that the vehicles converge to the common circle centered at the target with the given radius, as described in Γ_2. Fig. 4 illustrates that the vehicles converge to the evenly spaced formation independent of the number of vehicles, as described in Γ_3. Besides, the discontinuous points during 0-20s indicate that switchings of the sensor graph have occurred. Fig. 5 shows that $u_i(t) > \sup \|\dot{\boldsymbol{c}}\|$ and $u_i(t)$ converges to u_c. These results verify effectiveness of the proposed controller.

V. Conclusion

In this note, we have developed a cooperative controller for multiple nonholonomic vehicles, such that vehicles converge to an evenly spaced circular formation around a target moving with a time-varying velocity. The proposed controller only requires each vehicle to measure the information of its neighbors and the target in its local coordinate frame. Our future work will focus on vehicles with limited local measurements and analysis on collision avoidance.

References

[1] K.-K. Oh, M.-C. Park, and H.-S. Ahn, "A survey of multi-agent formation control," *Automatica*, vol. 53, pp. 424–440, 2015.

[2] N. E. Leonard, D. A. Paley, F. Lekien, R. Sepulchre, D. M. Fratantoni, and R. E. Davis, "Collective motion, sensor networks, and ocean sampling," *Proc. IEEE*, vol. 95, no. 1, pp. 48–74, 2007.

[3] J. A. Marshall, M. E. Broucke, and B. A. Francis, "Formations of vehicles in cyclic pursuit," *IEEE Trans. Autom. Control*, vol. 49, no. 11, pp. 1963–1974, 2004.

[4] ——, "Pursuit formations of unicycles," *Automatica*, vol. 42, no. 1, pp. 3–12, 2006.

[5] R. Sepulchre, D. A. Paley, and N. E. Leonard, "Stabilization of planar collective motion: All-to-all communication," *IEEE Trans. Autom. Control*, vol. 52, no. 5, pp. 811–824, 2007.

[6] ——, "Stabilization of planar collective motion with limited communication," *IEEE Trans. Autom. Control*, vol. 53, no. 3, pp. 706–719, 2008.

[7] N. Ceccarelli, M. Di Marco, A. Garulli, and A. Giannitrapani, "Collective circular motion of multi-vehicle systems," *Automatica*, vol. 44, no. 12, pp. 3025–3035, 2008.

[8] Y. Lan, G. Yan, and Z. Lin, "Distributed control of cooperative target enclosing based on reachability and invariance analysis," *Syst. Control Lett.*, vol. 59, no. 7, pp. 381–389, 2010.

[9] Z. Chen and H.-T. Zhang, "No-beacon collective circular motion of jointly connected multi-agents," *Automatica*, vol. 47, no. 9, pp. 1929–1937, 2011.

[10] ——, "A remark on collective circular motion of heterogeneous multi-agents," *Automatica*, vol. 49, no. 5, pp. 1236–1241, 2013.

[11] M. I. El-Hawwary and M. Maggiore, "Distributed circular formation stabilization for dynamic unicycles," *IEEE Trans. Autom. Control*, vol. 58, no. 1, pp. 149–162, 2013.

[12] R. Zheng, Y. Liu, and D. Sun, "Enclosing a target by nonholonomic mobile robots with bearing-only measurements," *Automatica*, vol. 53, pp. 400–407, 2015.

[13] T.-H. Kim and T. Sugie, "Cooperative control for target-capturing task based on a cyclic pursuit strategy," *Automatica*, vol. 43, no. 8, pp. 1426–1431, 2007.

[14] J. Guo, G. Yan, and Z. Lin, "Local control strategy for moving-target-enclosing under dynamically changing network topology," *Syst. Control Lett.*, vol. 59, no. 10, pp. 654–661, 2010.

[15] L. Ma and N. Hovakimyan, "Vision-based cyclic pursuit for cooperative target tracking," *J. Guid. Control Dynam.*, vol. 36, no. 2, pp. 617–622, 2013.

[16] J. O. Swartling, I. Shames, K. H. Johansson, and D. V. Dimarogonas, "Collective circumnavigation," *Unmanned Syst.*, vol. 2, no. 03, pp. 219–229, 2014.

[17] S. Zhu, D. Wang, and C. B. Low, "Cooperative control of multiple UAVs for source seeking," *J. Intell. Rob. Syst.*, vol. 70, no. 1-4, pp. 293–301, 2013.

[18] ——, "Cooperative control of multiple UAVs for moving source seeking," *J. Intell. Rob. Syst.*, vol. 74, no. 1-2, pp. 333–346, 2014.

[19] E. W. Frew, D. A. Lawrence, and S. Morris, "Coordinated standoff tracking of moving targets using Lyapunov guidance vector fields," *J. Guid. Control Dynam.*, vol. 31, no. 2, pp. 290–306, 2008.

[20] T. H. Summers, M. R. Akella, and M. J. Mears, "Coordinated standoff tracking of moving targets: control laws and information architectures," *J. Guid. Control Dynam.*, vol. 32, no. 1, pp. 56–69, 2009.

[21] Y. Lan, Z. Lin, M. Cao, and G. Yan, "A distributed reconfigurable control law for escorting and patrolling missions using teams of unicycles," in *Proc. 49th IEEE Conf. Decis. Control*, Atlanta, GA, USA, 2010, pp. 5456–5461.

[22] L. Briñón-Arranz, A. Seuret, and C. Canudas-de-Wit, "Cooperative control design for time-varying formations of multi-agent systems," *IEEE Trans. Autom. Control*, vol. 59, no. 6, pp. 1439–1453, 2014.

[23] Y. Kanayama, Y. Kimura, F. Miyazaki, and T. Noguchi, "A stable tracking control method for an autonomous mobile robot," in *Proc. 1990 IEEE Int. Conf. Rob. Autom.*, Cincinnati, Ohio, USA, 1990, pp. 384–389.

[24] M. I. El-Hawwary and M. Maggiore, "Reduction theorems for stability of closed sets with application to backstepping control design," *Automatica*, vol. 49, no. 1, pp. 214–222, 2013.

[25] N. Rouche, P. Habets, M. Laloy, and A. M. Ljapunov, *Stability theory by Liapunov's direct method*. Springer-Verlag New York, Inc., 1977.

[26] G. Oriolo, A. De Luca, and M. Vendittelli, "WMR control via dynamic feedback linearization: design, implementation, and experimental validation," *IEEE Trans. Control Syst. Technol.*, vol. 10, no. 6, pp. 835–852, 2002.

[27] H. H. Liu and G. K. Pang, "Accelerometer for mobile robot positioning," *IEEE Trans. Ind. Appl.*, vol. 37, no. 3, pp. 812–819, 2001.